TECHNICAL ARTICLE

Parametric Evaluation and Optimization of Laser Machining of SS304 Using Response Surface Methodology

Vikas B. Magdum ⓘ, Jayant K. Kittur, and Sachin C. Kulkarni

This study presents parametric evaluation and optimization of laser machining parameters of austenitic stainless steel 304 (SS 304) sheet. SS304 is a substantial manufacturing material machined by laser machining. The central composite design (CCD) of the response surface methodology (RSM) was utilized for the design of the experimental plan. Laser power, cutting speed, gas pressure and pulse frequency were used as process parameters, whereas kerf width and kerf taper were measured as performance characteristics. The factor effects on kerf width and kerf taper were analyzed using a surface plot. A good degree of fit was shown by the developed regression model. The analysis of variance results reveals that cutting speed, laser power and gas pressure had contributions of 41.49, 31.71 and 16.71% on kerf width, and 31.23, 26.03 and 19.81% on kerf taper. The optimal machining conditions of kerf width found at laser power of 1800 W, cutting speed of 1000 mm/min, gas pressure of 1.30 bar and a pulse frequency of 1500 Hz and of kerf taper at laser power of 1800 W, cutting speed of 802 mm/min, gas pressure of 1.30 bar and a pulse frequency of 1500 Hz. The higher cutting speed and gas pressure and lower laser power and pulse frequency result in the smallest kerf width, while an increase in cutting speed up to mid-level, higher gas pressure and lower laser power and pulse frequency result in the lower kerf taper. A mathematical model was developed to govern the relationship between the process parameters and the kerf width and kerf taper. The kerf width and kerf taper during the laser machining procedure are optimized efficiently through this method. It is clearly revealed that the performance characteristics of the laser machining process can be optimized efficiently by this method.

1. Introduction

The laser machining procedure has an extensive variety of applications in diverse production procedures because of its benefits of cost efficacy and high machining quality through a high production rate (Ref 1, 2). All engineering materials with complex shapes and close tolerances are machined by laser machining (Ref 3, 4). The first laser was built by Theodore H. Maiman in 1960. The laser focused on the workpiece generates a very high temperature because of which the workpiece is melted. A high-pressurized gas was used for ejecting melted material and generating kerf. A graphic of laser machining is shown in Fig. 1.

The dimensional accuracy of the machined kerf depends upon kerf taper (K_t), kerf width (K_w) and kerf deviation (K_d). K_t

and K_w were measured along the sheet thickness and machined length, respectively. The quality of machining could be improved by the optimal selection of process parameters. K_t and K_w remain the crucial performance characteristics of the laser machining process. K_t and K_w are mostly associated with dimensional accuracy and the high quality of the machined part.

SS304 (ASTM A240) sheet is a vital engineering material and is used in about 50% of stainless steel production and utilization. SS304 was selected as the workpiece material for the experimentation. In particular, SS304 is a nonmagnetic austenitic stainless steel. It is mainly composed of chromium ($\sim 18\%$) and nickel ($\sim 10\%$) with iron and additional elements. These elements affect ferrite austenite equilibrium. The microstructure depends on thermal parameters through phase transformation. The microstructure is changed due to the high heat generated during laser machining. SS304 offers advantages which include its better mechanical strength, oxidation resistance, corrosion resistance, chemical resistance and excellent visual appeal in architecture. It has developed as the preferred manufacturing material. SS304 sheets are applicable in various applications in the food industry, electronics, automobile headers, screws, machinery components, spacecraft and army devices. SS304 is hardened at some point of machining and subsequently turns into a tough material for conventional machining. But it is efficiently machined by laser machining (Ref 5-7).

Vikas B. Magdum, Department of Mechanical Engineering, DKTE Society's Textile and Engineering Institute, Ichalkaranji, Maharashtra 416115, India; and **Jayant K. Kittur** and **Sachin C. Kulkarni**, Department of Mechanical Engineering, KLS Gogte Institute of Technology, Belagavi, Karnataka 590008, India. Contact e-mails: vbmagdum@rediffmail.com, jkk@git.edu, and sckulkarni@git.edu.
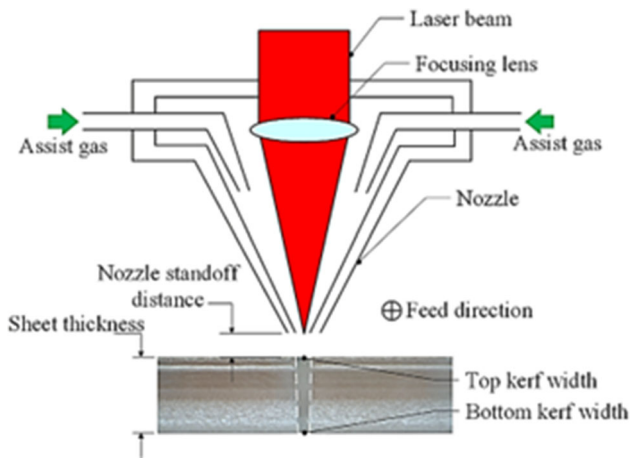
Fig. 1 Kerf geometry

2. Literature Review

A literature review was carried out to study significant process parameters and their effects on K_w and K_t and modeling and optimization methods. The laser machining process is categorized through various process parameters and their relations, which control the machining process effectivity. The effectivity of the process is measured in terms of productivity, quality and cost. These goals are achieved through the optimal selection of process parameters. In the industry, these process parameters are selected based on experience and a trial-and-error process. Such a way is time-consuming and does not give an optimal solution. Therefore, it is essential to accurately evaluate the relationship between process parameters and performance characteristics by mathematical modeling.

Elyas Haddadi et al. studied decreasing cutting speed and increasing laser power to cause an increase in kerf width (Ref 3). M. Moradi et al. found that the minimum taper obtained the lowest laser power and high frequency (Ref 4). Milos Madic et al. observed that the combination of low cutting speed and high gas pressure increases the energy supply to the workpiece surface and increases the kerf width considerably, and a decrease in the kerf width occurs with an increase in the cutting speed (Ref 8). Avanish Kumar Dubey et al. studied the consequences of process parameters on K_w, K_t and K_d. The appropriate selection of numerous process parameters could improve the machining quality of the cut (Ref 9). Arun Kumar Pandey et al. observed that pulse width was the utmost substantial parameter for K_w trailed by pulse frequency, gas pressure and cutting speed. A wider K_w was generated by an increase in pulse width. However, K_w was wider at a lower value of pulse frequency. Laser beam sheet metal interface time rises through an increase in pulse width to allow the transfer of absorbed heat to a bigger area, inflicting wider K_w. Then again, with the aid of reducing the pulse width and increasing peak power had a tendency to enter deeper with smaller heat conduction at edges because of the decreased beam and sheet metal interface time causing lower K_w. Higher pulse frequencies produce more pulse energy and result in deep penetration instead of melting more material from edges that generate reduced K_w. K_w increased up to a certain limit as pulse frequency increased and started reducing after that. Also, minimum K_w occurred at a lower pulse width (Ref 10). D.

Kondayya et al. noticed that the K_w becomes narrower by raising the cutting speed and widens with a rise in pulse energy and pulse frequency. The outcome of varying pulse energy was comparatively greater than pulse frequency on K_w (Ref 11). K.K. Mandal et al. observed that an increase in frequency and laser beam power reduces K_w. Because of the increase in laser power, more heat was generated. The maximum amount of heat was accountable for producing a wider K_w by removing more material from the workpiece. Also, K_w widens with the increase in pulse frequency (Ref 12). Bekir Sami Yilbas et al. expressed and anticipated the K_w dimensions by the lump parameter evaluation model. The difference in K_w size rises with increasing cutting speed and laser power (Ref 13). Teeraphat Kongcharoen et al. noticed the outcome of process parameters on K_w in laser machining of mild steel plate. The results showed that an increase in the laser power increased K_w. The average K_w becomes narrower with the increase in cutting speed (Ref 14). Statistical and mathematical tools were accumulated in response surface methodology (RSM). RSM is intended for modeling, optimizing and evaluating the outcome of process parameters on performance characteristics. Process optimization was carried out with a smaller number of experiments and high accuracy of results (Ref 3, 15). S. C. Kulkarni et al. applied RSM for evaluating the outcome of process parameters and the adequacy of the model was tested by analysis of variance (ANOVA) (Ref 16). A.M. Sifullah et al. observed that laser power is the most influenced parameter with a 64.21% contribution to the kerf width of HAZ. The laser beam intensity increases with an increase in laser power resulting in a wider width of HAZ. While laser material interaction time decreases with an increase in cutting speed, this results in a narrowing of the width of HAZ. (Ref 17). A. D. Tura et al. used a hybrid approach of GA and RSM for optimization and analysis of laser machining parameters on SS304 (Ref 18). Mahmoud Moradi et al. found that as the cutting speed decreases and laser power increases, more heat input was supplied to the material resulting in more area of the material being heated and melted; therefore, the kerf width will become wider (Ref 19).

Conferring to the literature, there has not been an inclusive study on the laser machining of the SS304 sheet. SS304 has wide applications in the industry. So, it seems important to study the laser machining of SS304, to produce high-quality and more accurate components. The objective of this work is to develop the model for optimizing and evaluating the numerous process parameter effects, for instance, the cutting speed, laser power, gas pressure and pulse frequency on the K_w and K_t for achieving precise laser machining. The central composite design (CCD) of the response surface methodology is utilized for the design of the experimental plan. A mathematical model based on response surface methodologies was used for the optimization of kerf width and kerf taper. The factor effects on kerf width and kerf taper are analyzed using a surface plot.

3. Experimental Setup

Experiment runs were conducted with a 2.5 K_w AMADA F0MTII3015 laser machine provided by Merasha Shapers Pvt. Ltd., Maharashtra, India. The machining was performed on a 5-mm-thick SS304 sheet. The chemical composition of SS304 is shown in Table 1.

Table 1 Chemical composition of SS304

% C	% Mn	% S	% P	% Si	% Ni	% Cr	% N
0.06	0.86	0.002	0.04	0.28	8.01	18.01	0.04

Fig. 2 Experimental setup

Table 2 Process parameters

Sr. No	Process parameter	Level		
		− 1	0	1
1	Laser power (W)	1800	2150	2500
2	Cutting speed (mm/min)	600	800	1000
3	Gas pressure (bar)	0.9	1.1	1.3
4	Pulse frequency (Hz)	1500	1750	2000

Fig. 3 Machined workpiece

Fig. 4 Kerf width measurement setup

A photographic image of the experimental setup is displayed in Fig. 2.

The process parameters selected that affect the K_w and K_t were based totally on the literature review, machine specification and pilot experimentation. Through the above study, 4 parameters at 3 levels that mainly have an effect on the K_w and K_t have been decided. As for laser power, cutting speed, gas pressure and pulse frequency, they were taken into consideration as process parameters. In Table 2, laser machining process parameters along with machining levels were revealed.

The relationship among laser machining process parameters (cutting speed, laser power, gas pressure and pulse frequency) and the performance characteristics (K_w and K_t) was obtained from the RSM approach. Experimental effects, attained from the RSM experimental plan, have been used for evolving predictive models. The goal of this method was to simultaneously look for the optimum set of parameters so that this method is capable of appropriately modeling the laser machining process. Experiments are planned by applying the central composite design (CCD) of RSM. The interactive and higher-order effects are studied through the laser machining of SS304 by RSM. The ANOVA was used to test the adequacy of the established model. The laser machining parameters will be optimized for high machining accuracy and production. The effects of process parameters such as cutting speed, laser power, gas pressure and pulse frequency on K_w and K_t were evaluated and optimized. Straight cuts of 10 mm in length were machined as per the experimental run. The machining shape was designed with the aim of allowing the measurement of the kerf width in an easy and precise way. K_w is of two types: top and bottom K_w. Top and bottom K_w was measured along the machined length with a 10X magnification microscope at the top and bottom surfaces, respectively. The machined workpiece and the measurement setup are shown in Figs. 3 and 4, respectively.

Kerf taper is an important parameter determined by the top and bottom kerf width and workpiece thickness. Equation 1 is used for calculating the K_t

$$\text{Kerf taper } (K_t^\circ) = \frac{(\text{Top kerf width} - \text{Bottom kerf width}) \times 180}{2\pi \times \text{Thickness of workpiece}}$$

(Eq 1)

A central composite design of RSM was planned for an experimental run to study the relationship among the process parameters and performance characteristics revealed in Table 3. A total of 93 experiments with 3 replicates were performed.

Table 3 Experimental plan and observed K_w and K_t

Exp run	Laser power	Cutting speed	Gas pressure	Pulse frequency	K_w	K_t
1	1	1	1	1	0.253	0.178
2	− 1	0	0	0	0.238	0.132
3	0	0	0	0	0.277	0.229
4	0	1	0	0	0.239	0.218
5	0	0	0	0	0.284	0.263
6	1	− 1	− 1	1	0.485	0.997
7	− 1	0	0	0	0.243	0.120
8	1	1	1	− 1	0.251	0.183
9	− 1	1	1	− 1	0.212	0.172
10	− 1	− 1	1	− 1	0.235	0.155
11	0	0	0	− − 1	0.262	0.206
12	1	− 1	− 1	− 1	0.434	0.762
13	− 1	1	− 1	− 1	0.219	0.149
14	1	− 1	1	1	0.388	0.533
15	0	0	0	0	0.290	0.338
16	− 1	− 1	− 1	− 1	0.348	0.412
17	0	0	0	0	0.292	0.332
18	1	− 1	1	− 1	0.378	0.441
19	1	0	0	0	0.363	0.458
20	0	0	0	0	0.295	0.304
21	1	1	− 1	1	0.336	0.412
22	0	− 1	0	0	0.372	0.504
23	− 1	1	1	1	0.212	0.166
24	1	1	− 1	1	0.341	0.412
25	0	0	0	0	0.299	0.315
26	0	0	0	0	0.296	0.298
27	− 1	0	0	0	0.239	0.120
28	− 1	1	1	1	0.219	0.223
29	0	0	0	0	0.305	0.321
30	0	0	0	0	0.307	0.309
31	0	0	0	0	0.304	0.326
32	1	1	1	− 1	0.244	0.132
33	0	0	1	0	0.250	0.115
34	− 1	− 1	− 1	1	0.356	0.470
35	1	− 1	1	− 1	0.383	0.452
36	0	0	0	0	0.309	0.338
37	1	1	− 1	− 1	0.327	0.361
38	− 1	1	1	− 1	0.207	0.162
39	0	0	0	1	0.331	0.384
40	− 1	− 1	1	− 1	0.233	0.109
41	1	− 1	1	− 1	0.389	0.475
42	0	0	− 1	0	0.343	0.424
43	0	− 1	0	0	0.381	0.538
44	1	0	0	0	0.370	0.515
45	0	0	0	0	0.313	0.315
46	0	0	− 1	0	0.345	0.424
47	− 1	1	− 1	− 1	0.222	0.155
48	− 1	− 1	1	1	0.273	0.241
49	− 1	1	− 1	1	0.231	0.172
50	0	0	1	0	0.251	0.137
51	0	0	0	− 1	0.268	0.218
52	0	− 1	0	0	0.382	0.504
53	1	0	0	0	0.372	0.550
54	1	− 1	1	1	0.395	0.538
55	− 1	1	− 1	1	0.234	0.172
56	0	0	0	1	0.335	0.418
57	1	1	− 1	1	0.344	0.418
58	0	0	0	0	0.311	0.292
59	0	0	0	0	0.315	0.361
60	− 1	− 1	1	− 1	0.240	0.132
61	− 1	1	1	− 1	0.198	0.155
62	0	0	− 1	0	0.351	0.435
63	− 1	− 1	− 1	− 1	0.353	0.407
64	0	0	0	0	0.321	0.384

Table 3 continued

Exp run	Laser power	Cutting speed	Gas pressure	Pulse frequency	K_w	K_t
65	0	0	0	1	0.337	0.452
66	0	0	1	0	0.255	0.189
67	1	− 1	− 1	1	0.492	1.019
68	− 1	− 1	1	1	0.275	0.218
69	− 1	1	− 1	1	0.235	0.143
70	1	1	− 1	− 1	0.331	0.401
71	− 1	− 1	− 1	1	0.359	0.441
72	− 1	− 1	− 1	− 1	0.355	0.412
73	1	− 1	1	1	0.398	0.544
74	0	1	0	0	0.233	0.160
75	0	0	0	0	0.317	0.355
76	0	0	0	0	0.321	0.344
77	1	1	1	− 1	0.245	0.115
78	1	− 1	− 1	− 1	0.434	0.756
79	0	0	0	0	0.324	0.344
80	1	− 1	− 1	1	0.471	0.945
81	− 1	1	1	1	0.221	0.166
82	0	0	0	0	0.318	0.321
83	− 1	− 1	− 1	1	0.364	0.464
84	0	0	0	0	0.324	0.401
85	0	0	0	0	0.327	0.361
86	− 1	1	− 1	− 1	0.230	0.160
87	− 1	− 1	1	1	0.279	0.235
88	1	1	1	1	0.249	0.137
89	1	1	− 1	− 1	0.333	0.441
90	1	1	1	1	0.247	0.115
91	0	1	0	0	0.233	0.137
92	0	0	0	− 1	0.270	0.206
93	1	− 1	− 1	− 1	0.440	0.682

4. Results and Discussion

Process parameters and their effects were discussed in this section. A better sense of the relative impact of the one-of-a-kind parameter may be acquired with the aid of the decomposition of the variance, which is known as ANOVA. This is a statistical approach used to evaluate the contribution of process parameters to K_w and K_t. The adequacy of the model was tested by ANOVA, which also calculates the significance of coefficients. The ANOVA results were counted at a 95% of a significance level. The ANOVA results for K_w and K_t are enumerated in Tables 4 and 5, respectively. The higher F values of 99.4 and 88.89 of K_w and K_t, respectively, indicate that the generated model was found to be significant and adequate for K_w and K_t. Tables 4 and 5 also showed significant and nonsignificant parameters. The parameters having p values less than 0.05 considered significant. The probability value in the model represents the effect of different terms. Percentage contribution or F ratio represents the relative significance of a corresponding factor. A higher value of the F ratio indicates a more significant parameter.

The Minitab 17 software was used to evaluate the K_w and K_t. For the K_w and K_t models, the ANOVA indicates that the cutting speed, laser power and gas pressure are having more significant effects on K_w and K_t. The interaction effect and square effect of process parameters are less significant than linear effects of process parameter. The RSM was applied to evaluate the relationship among different process parameters. The lower the better value is the optimum for K_w and K_t. The

RSM methodology uses a scientific process to correlate the process parameters with the K_w and K_t and form a second-order polynomial equation. The generated model enumerates the relationships and evaluates the linear, square and interaction effects of process parameters on the performance characteristics. This model helps to study the behavior of processes. A model was developed for the response surface to analyze the influence of process parameters on the K_w and K_t. The Minitab 17 software is used to formulate the regression equation considering significant parameters only and compute the coefficients for K_w and K_t are shown in Eq 2 and 3, respectively. Insignificant model parameters can be eliminated through the step-wise regression method.

$$\begin{aligned} \text{Kerf width } (K_w) = {} & 0.357 + 0.000221A - 0.000511\,B - 0.1882\,C \\ & + 0.000046\,D - 0.000073\,A*C \\ & + 0.000208\,B*C \end{aligned}$$

(Eq 2)

$$\begin{aligned} \text{Kerf taper } K_t = {} & -1.974 + 0.001879\,A - 0.000542\,B \\ & + 0.021\,C + 0.000603\,D + 0.000001\,B \\ & *B - 0.000001\,A*B - 0.000696\,A*C \\ & + 0.001146\,B*C - 0.000001\,B*D \end{aligned}$$

(Eq 3)

where A, B, C and D are laser power, cutting speed, gas pressure and pulse frequency, respectively.

Table 4 ANOVA results for kerf width

Source	DF	Adj SS	Adj MS	F-Value	P Value	Contr %
Model	14	0.392181	0.028013	99.4	0.000	94.69
Linear	4	0.379432	0.094858	336.58	0.000	91.61
A	1	0.131325	0.131325	465.97	0.000	31.71
B	1	0.171817	0.171817	609.65	0.000	41.49
C	1	0.069194	0.069194	245.52	0.000	16.71
D	1	0.007096	0.007096	25.18	0.000	1.71
Square	4	0.000779	0.000195	0.69	0.600	0.19
A*A	1	0.000067	0.000067	0.24	0.626	0.02
B*B	1	0.00023	0.00023	0.82	0.369	0.06
C*C	1	0.000033	0.000033	0.12	0.733	0.01
D*D	1	0.000004	0.000004	0.01	0.904	0.00
2-Way Interaction	6	0.01197	0.001995	7.08	0.000	2.89
A*B	1	0.00644	0.00644	22.85	0.000	1.55
A*C	1	0.001261	0.001261	4.47	0.038	0.30
A*D	1	0.00000	0.00000	0	0.973	0.00
B*C	1	0.003333	0.003333	11.83	0.001	0.80
B*D	1	0.000919	0.000919	3.26	0.075	0.22
C*D	1	0.000016	0.000016	0.06	0.810	0.00
Error	78	0.021983	0.000282			5.31
Lack-of-Fit	10	0.016955	0.001695	22.93	0.000	4.09
Pure Error	68	0.005028	0.000074			1.21
Total	92	0.414164				100.00

Table 5 ANOVA results for kerf taper

Source	DF	Adj SS	Adj MS	F- Value	P Value	Contri %
Model	14	3.21054	0.22932	95.68	0.000	94.50
Linear	4	2.7086	0.67715	282.51	0.000	79.72
A	1	0.88448	0.88448	369.01	0.000	26.03
B	1	1.0611	1.0611	442.70	0.000	31.23
C	1	0.67313	0.67313	280.83	0.000	19.81
D	1	0.08989	0.08989	37.5	0.000	2.65
Square	4	0.03715	0.00929	3.87	0.006	1.09
A*A	1	0.00085	0.00085	0.36	0.552	0.03
B*B	1	0.01133	0.01133	4.73	0.033	0.33
C*C	1	0.00257	0.00257	1.07	0.304	0.08
D*D	1	0.00057	0.00057	0.24	0.627	0.02
2-Way Interaction	6	0.4648	0.07747	32.32	0.000	13.68
A*B	1	0.20546	0.20546	85.72	0.000	6.05
A*C	1	0.11393	0.11393	47.53	0.000	3.35
A* D	1	0.00557	0.00557	2.33	0.131	0.16
B*C	1	0.10093	0.10093	42.11	0.000	2.97
B*D	1	0.03625	0.03625	15.12	0.000	1.07
C*D	1	0.00265	0.00265	1.11	0.296	0.08
Error	78	0.18696	0.0024			5.50
Lack-of-Fit	10	0.12327	0.01233	13.16	0.000	3.63
Pure Error	68	0.06369	0.00094			1.87
Total	92	3.3975				100.00

The ability of generated models (Eq 2 and 3) to represent machining processes is shown by ANOVA results. The ANOVA results showed the significance of linear terms A, B, C, D, square terms of A, B, C and D and the interaction terms AB, AC, AD, BC, BD, CD. For the kerf width model, the ANOVA indicates that the linear effects of all process parameters and the interaction effect between AC and BC are the significant model terms. While for the kerf taper model, the ANOVA indicates that the linear effect of all process param-eters, the square effect of B and the interaction effect between AB, AC, BC and BD are the significant model terms. Cutting speed, laser power and gas pressure contributed 41.39, 31.71 and 16.71% to K_w and 31.23, 26.03 and 19.81% to K_t. The R^2 and Adj. R^2 values for K_w are achieved to be 94.28% and 93.81%, respectively, and for K_t 94.5 and 93.51%, respectively. These high values show a high correlation among the observed values and the predicted values. The deviation among R^2 and predicted R^2 value is smaller. The lack-of-fit value was not

significant indicating a good-fitting model was preferred. The acceptable precision and adequacy index indicate a high accuracy level of the experimental data used in constructing a model. The normal probability plots for K_w and K_t shown in Figs. 5 and 6 indicate that the obtained model was practically acceptable. It showed that the residuals were close to straight line, indicating that good pattern and normal structure were found and the errors were normally distributed, supporting that the parameters considered in the established models were significant. Overall, the statistical study replicates that the experimental values and predicted values were well fitted for the preferred range of process parameters and the accuracy of the model was found adequate.

Minitab 17 statistical software was used for the analysis using the main effects plot shown in Figs. 7 and 8 for K_w and K_t, respectively. Both K_w and K_t show a similar pattern for the main effects plot. The study depends on mathematical models and experimental results developed using RSM and ANOVA. The main effects plot shows increasing cutting speed results in decreasing K_w and K_t. Because of higher cutting speed, less the energy density provided to the workpiece results in less time used for the heat to melt edges and thus narrower the K_w and smaller K_t generated. As cutting speed increases, less power density provided to the metal sheet. During this small-time heat was diffused to sideways and a narrower kerf was produced. A higher laser power supplied considerable heat to the workpiece

material and wider kerfs and larger K_t were produced. An increase in pulse frequency had a tendency to lower the interface time between workpiece and heat which results in less dispersion of heat. Therefore, K_w and K_t increase with an increase in pulse frequency. A higher gas pressure expels the melted material from the workpiece offering a cool cut and producing a narrower K_w.

The response surface plots of parameters for K_w are shown in Fig. 9. Process parameter values are maintained at the mid-level. In Fig. 9(a), cutting speed and pulse frequency values were kept constant at 800 mm/min and 1750 Hz. K_w increases with a decrease in cutting speed and an increase in laser power. However, the result of varying cutting speeds on K_w was more lead than laser power. At high cutting speed and low laser power, the machining process was more reliable and had consequences in low K_w. The effect of laser power and gas pressure is given in Fig. 9(b). It indicates K_w increased by an increase in laser power and a decrease in gas pressure. At high laser power and low gas pressure more heat is supplied to the sheet and molten metal is not removed quickly, so K_w increases. Figure 9(c) exhibits the significance of laser power and pulse frequency on K_w. It was increased with an increase in laser power and pulse frequency. Laser power was having more impact on K_w compared to pulse frequency. Figure 9(d) exhibits the intent of cutting speed and gas pressure on K_w. It was increased with a decrease in cutting speed and gas
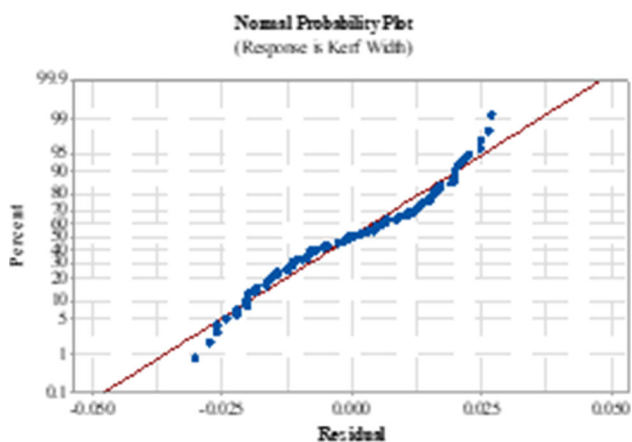

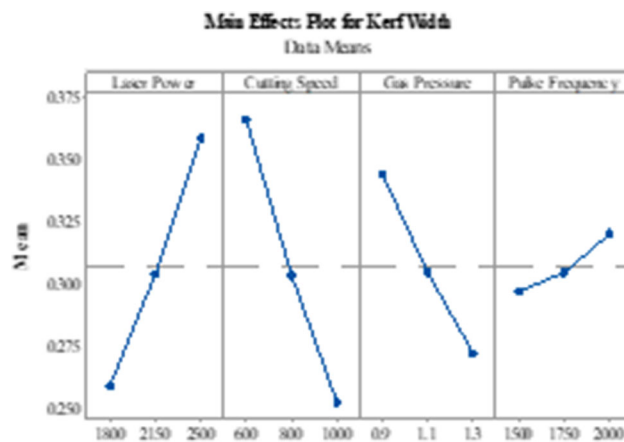**Fig. 5** Normal probability plot for K_w
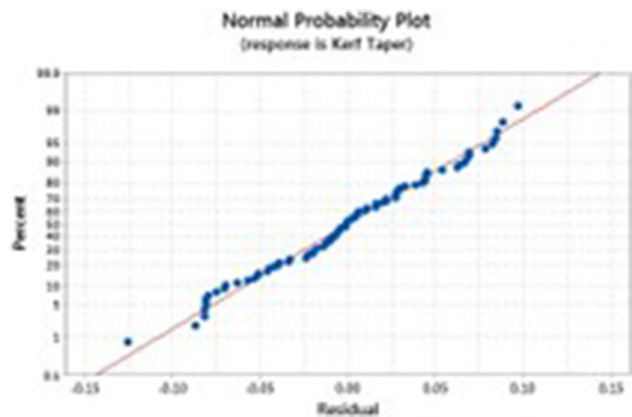

Fig. 7 Main effects plot for K_w

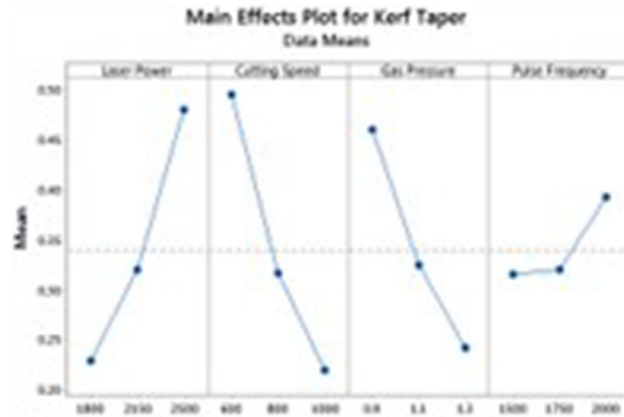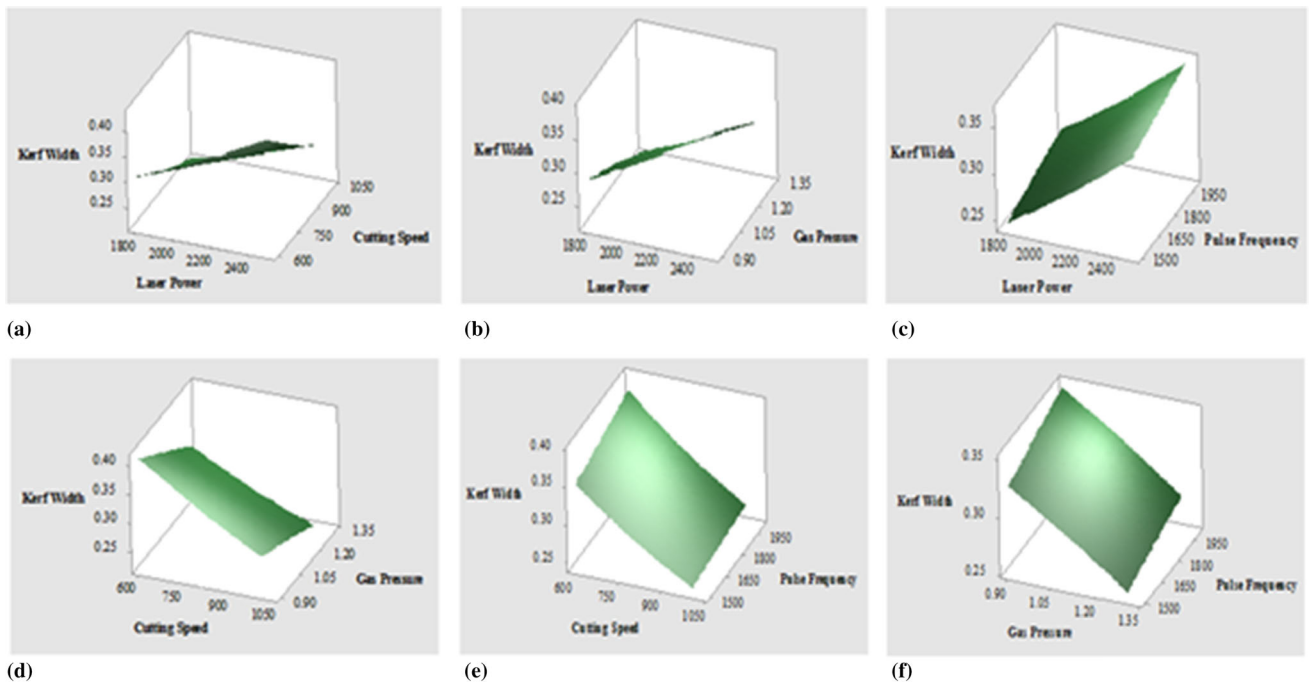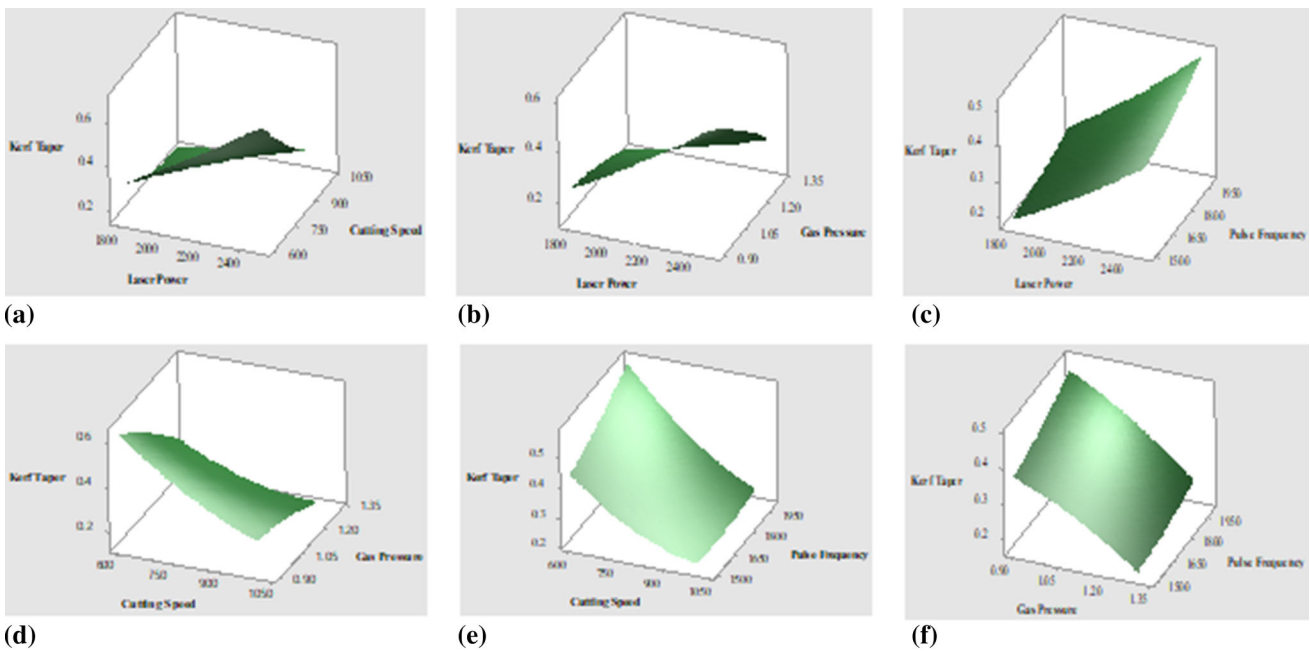**Fig. 6** Normal probability plot for K_t

Fig. 8 Main effects plot for K_t

Fig. 9 Surface plot for K_w: (a) laser power vs. cutting speed (b) gas pressure vs. laser power (c) pulse frequency vs. laser power (d) gas pressure vs. cutting speed (e) cutting speed vs. pulse frequency (f) gas pressure vs. pulse frequency

Fig. 10 Surface plot for K_t: (a) laser power vs. cutting speed (b) gas pressure vs. laser power (c) pulse frequency vs. laser power (d) gas pressure vs. cutting speed (e) cutting speed vs. pulse frequency (f) gas pressure vs. pulse frequency

pressure. At higher cutting speeds and gas pressure, less time is offered for heat diffusion and melting hence lower K_w. Figure 9(e) shows the influence of cutting speed and pulse frequency on K_w. It was increased with a decrease in cutting speed and an increase in pulse frequency. At high cutting speed and low pulse frequency, the amount of heat supplied was limited, and thus, a lower K_w was produced. Figure 9(f) shows the impact of pulse frequency and gas pressure on K_w. It was increased with an increase in pulse frequency and gas pressure.

At low levels of pulse frequency and high levels of gas pressure, the thermal energy incident on the sheet was to a small extent, resulting in lower K_w.

The response surface plots of parameters for K_t are shown in Fig. 10. Process parameter values were maintained at the mid-level. Figure 10(a) evinces that an increase in laser power results in an increase in K_t and K_t increases with increase in cutting speed up to about mid-level and again increases with increase in cutting speed. It was slightly decreasing at mid
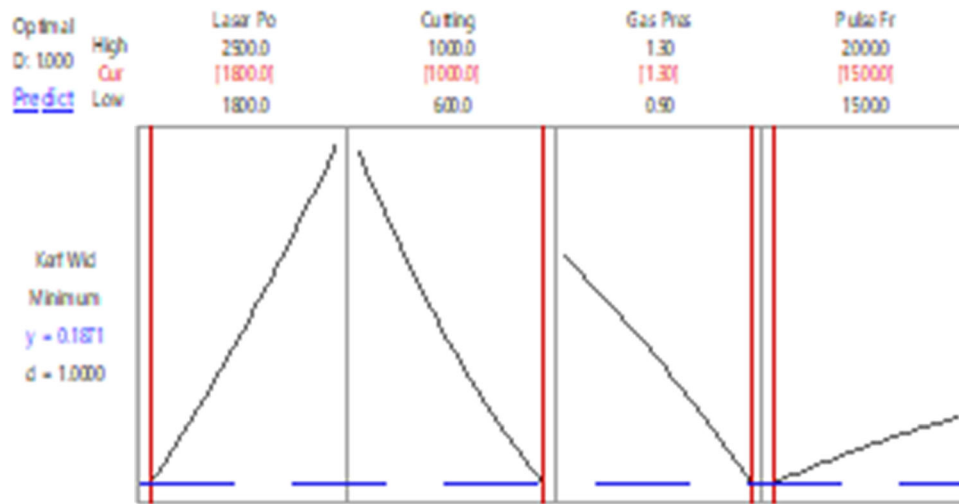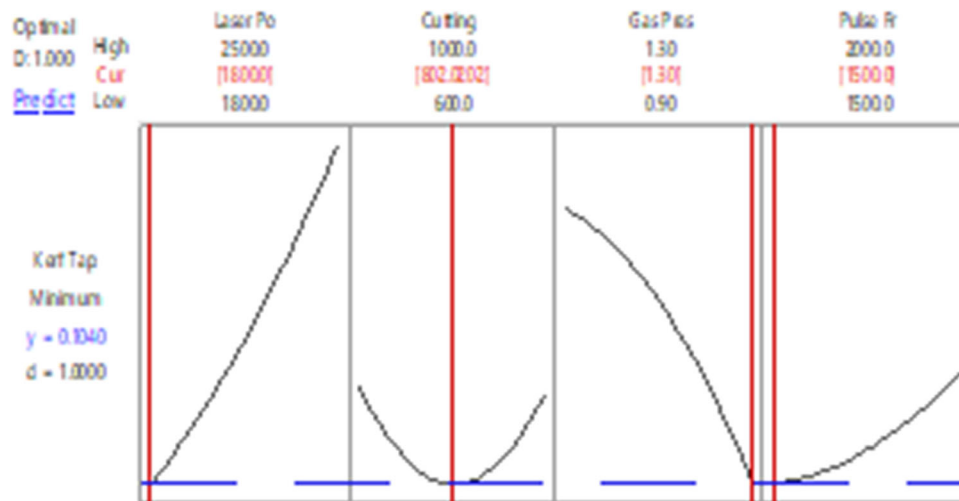
Fig. 11 Optimality plot of K_w

Fig. 12 Optimality plot of K_t

values. The combined effect of laser power and gas pressure is shown in Fig. 10(b). K_t increases with a decrease in gas pressure and an increase in laser power. Figure 10(c) shows that melting and resolidification increase with higher values of pulse frequency and result in K_t increases. Figure 10(d) shows cutting speed was more significant than gas pressure. Higher gas pressure ejects melted material from the machined kerf, contributing to cool cutting and smaller K_t. As shown in Fig. 10(e), a lower cutting speed and lower pulse frequency can provide more energy to the workpiece, resulting in an increase in K_t. Figure 10(f) exhibits K_t increase with a decrease in gas pressure and an increase in pulse frequency. Gas pressure was the more significant parameter as compared to pulse frequency on K_t.

Optimal plot of K_w and K_t is shown in Figs. 11 and 12, respectively. Figure 11 indicates that minimum K_w found at laser power of 1800 W, cutting speed of 1000 mm/min, gas pressure of 1.30 bar and a pulse frequency of 1500 Hz and minimum Figure 12 indicates that K_t found at laser power of 1800 W, cutting speed of 826.26 mm/min, gas pressure of 1.30 bar and a pulse frequency of 1500 Hz.

An increase in laser power leads to higher K_w and K_t resulting in the reduction of machined kerf quality. At higher laser power, if gas pressure is not increased, more molten material is ejected toward the top of the interaction zone and melts additional material, resulting in a large kerf. Higher gas pressure easily ejected molten material from the machined kerf. At higher cutting speeds, less energy is provided to the workpiece material, less time is available for melting and heat diffusion and hence produces lower K_w. But K_t first decreases with an increase in cutting speed up to mid-level and then increases with increase in cutting speed. At a lower pulse frequency, the machining process is steadier and results in low K_w and K_t. Pulse frequency is directly proportional to pulse energy. Due to the low pulse frequency, more time is available to cooling down the material. At high pulse frequencies, the intense melting and vaporization produce a wider K_w and higher K_t. Also, resolidification and dross formation will increase with an increase in pulse frequency. Main effects plot shows that process parameters became more significant from middle to higher levels.

5. Conclusion

This work optimized and evaluated the effects of the process parameters during laser machining of a 5-mm sheet of SS304 by using the CCD of RSM and ANOVA. The following outcomes can be concluded from this work:

- The central composite design of RSM was used to design an experiment and a regression model evaluating the relationship between K_w, K_t, and process parameters were developed. The developed model was tested by ANOVA and found adequate. The experimental values and predicted values were well fitted with an R^2 value of 94.69% and 94.50% for K_w and K_t, respectively.
- A high cutting speed and gas pressure and low laser power and pulse frequency result in a decrease in K_w and K_t. A low laser power generates less heat, a high cutting speed results in a concentration of heat for less time, high gas pressure would eject the molten metal from the kerf and contribute to a cool cut, and a low pulse frequency avoids excessive melting and resolidification resulting in lower K_w and K_t. An increase in laser power and pulse frequency and a decrease in cutting speed and gas pressure increase the kerf width. Also, increase in laser power and pulse frequency and a decrease in gas pressure increase the kerf taper. But kerf taper first decreases with an increase in cutting speed up to mid-level and then increases with increases in cutting speed.
- The cutting speed, laser power and gas pressure had a contribution of 41.39, 31.71 and 16.71% on the K_w and 31.23, 26.03 and 19.81% on the K_t. The cutting speed was observed to be the most influenced process parameter in this machining range.
- RSM was used to identify optimal parameters in the laser machining of SS304. The optimal machining conditions of K_w found at laser power of 1800 W, cutting speed of 1000 mm/min, gas pressure of 1.30 bar and a pulse frequency of 1500 Hz and of K_t at laser power of 1800 W, cutting speed of 802 mm/min, gas pressure of 1.30 bar and a pulse frequency of 1500 Hz.
- This work showed that the proposed optimization method is effective in optimizing the process and analyzing the effects of process parameters on performance characteristics. This method is applicable for development in the laser machining industry by improving machining quality through suitable selection of process parameters. This method can provide an essential basis for manufacturers using laser machining technology.

References

1. H.A. Eltawahni, M. Hagino, K.Y. Benyounis, T. Inoue, and A.G. Olabi, Effect of CO2 Laser Cutting Process Parameters on Edge Quality and Operating Cost of AISI316L, *Opt. Laser Technol.*, 2012, **44**, p 1068–1082.
2. R. Surebana, V.N. Kulkarni, and V.N. Gaitonde, Modern Optimization Techniques for Advanced Machining Processes–A Review, *Mater. Today: Proc.*, 2019, **18**, p 3034–3042.
3. E. Haddadi and M. Moradi, Ayub Karimzad Ghavidel, Ali Karimzad Ghavidel, Saleh Meiabadi, Experimental and Parametric Evaluation of Cut Quality Characteristics in CO2 Laser Cutting of Polystyrene, *Optik*, 2021, **184**, p 103–114.
4. M. Moradi and H. Abdollahi, Statistical Modelling and Optimization of the Laser Percussion Microdrilling of Thin Sheet stainless Steel, *Lasers Eng.*, 2018, **40**(4–6), p 375–393.
5. D.J. Kotadiya and D.H. Pandya, Parametric Analysis of Laser Machining with Response Surface Method on SS-304, *Procedia Technol.*, 2016, **23**, p 376–382.
6. M. Sarıkaya and V. Yılmaz, Optimization and Predictive Modeling Using S/N, RSM, RA and ANNs for Micro-Electrical Discharge Drilling of AISI 304 Stainless Steel Springer, *Neural Comput. Appl.*, 2018, **30**, p 1503–1517.
7. D.F. Pessoa, P. Herwig, A. Wetzig, and M. Zimmermann, Influence of Surface Condition due to Laser Beam Cutting on the Fatigue Behavior of Metastable Austenitic Stainless Steel AISI 304 Elsevier, *Eng. Fract. Mech.*, 2017, **185**, p 227–240.
8. M. Madic and M. Radovanovic, Application of RCGA-ANN Approach for Modeling K_w and Surface Roughness in CO2 Laser Cutting of Mild Steel, *J. Braz. Soc. Mech. Sci. Eng.*, 2013, **35**, p 103–110.
9. Avanish Kumar Dubey, Vinod Yadava, Multi-Objective Optimization of Nd:YAG Laser Cutting of Nickel-Based Superalloy Sheet Using Orthogonal Array with Principal Component Analysis, Elsevier, *Opt. Lasers Eng.*, 2008, **46**, p 124–132.
10. Arun Kumar Pandey, Avanish Kumar Dubey, "Multiple Quality Optimization in Laser Cutting of Difficult-to-Laser-cut Material Using Grey-Fuzzy Methodology," *Int. J. Adv. Manuf. Technol.*, 2013, **65**, p 421–431.
11. D. Kondayya and A. Gopala Krishna, An Integrated Evolutionary Approach for Modelling and Optimization of Laser Beam Cutting Process Springer, *Int. J. Adv. Manuf. Technol.*, 2013, **65**, p 259–274.
12. K.K. Mandal, A.S. Kuar, and S. Mitra, Experimental Investigation on Laser Micro-Machining of Al 7075 Al, *Opt. Laser Technol.*, 2018, **107**, p 260–267.
13. Bekir Sami Yilbas, Mian Mobeen Shaukat, Farhan Ashraf, "Laser Cutting of Various Materials: Kw size Analysis and Life Cycle Assessment of Cutting Process", Elsevier, *Opt. Laser Technol.*, 2017, **93**, p 67–73.
14. T. Kongcharoen and M. Suchatawat, Effects of the Laser Process Parameters on Kerf Quality, *Int. J. Mech. Eng. Robot. Res.*, 2018, **7**(2), p 164–168.
15. A. Ghosal and A. Manna, Response surface Method Based Optimization of Ytterbium Fiber Laser Parameter During Machining of Al/Al2O3-MMC Elsevier, *Opt. Laser Technol.*, 2013, **46**, p 67–76.
16. S.C. Kulkarni, M.S. Patil, A.V. Kulkarni, R.M. Kulkarni, and R.R. Malagi, Effect of Manufacturing Method of Cu-Al Electrode on Performance During Electric Discharge Machining of Siliconised Silicon Carbide (SiSiC), *Mater. Today: Proc.*, 2020, **27**, p 120–129.
17. A.M. Sifullah, A. Khaled, Y. Nukman, M.A. Hassan, and A. Hossain, Laser Cutting of Square Blanks in Stainless Steel-304 Sheets: HAZ and Thermal Stress Analysis, *Sains Malays.*, 2017, **46**(5), p 755–762.
18. A.D. Tura, H.B. Mamo, and D.G. Desisa, Multi-Objective Optimization and Analysis for Laser Beam Cutting of Stainless Steel (SS304) Using Hybrid Statistical Tools GA-RSM, *IOP Conf. Ser. Mater. Sci. Eng.*, 2021, **1201**(1), p 012030.
19. M. Moradi, O. Mehrabi, T. Azdast, and K.Y. Benyounis, Enhancement of Low Power CO2 laser Cutting Process for Injection Molded Polycarbonate, *Opt. Laser Technol.*, 2017, **96**, p 208–218.